Final published version of this article: PHYSICAL REVIEW B 90, 201401(R) (2014)
DOI: https://doi.org/10.1103/PhysRevB.90.201401

Metallic picene/C60 heterojunctions and the effect of potassium doping

Marco Caputo, Mirco Panighel, Luca Petaccia, Claudia Struzzi, and Vajiheh Alijani
Elettra Sincrotrone Trieste, s.s. 14 km 163.5 in Area Science Park, 34149 Trieste, Italy

Marcello Coreno
CNR-IMIP, Montelibretti, Roma, Italy

Monica de Simone
TASC CNR-IOM Laboratory, s.s. 14 km 163.5 in Area Science Park, 34169 Trieste, Italy

Guido Fratesi
ETSF, CNISM, and Dipartimento di Scienza dei Materiali, Università Milano-Bicocca, via Cozzi 55, 20125 Milano, Italy
and Dipartimento di Fisica, Università di Milano, via Celoria 16, 20133 Milano, Italy

Giovanni Di Santo and Andrea Goldoni*
Elettra Sincrotrone Trieste, s.s. 14 km 163.5 in Area Science Park, 34149 Trieste, Italy and INSTM–Elettra, Micro & Nano-Carbon
Laboratory, s.s. 14 km 163.5 in Area Science Park, 34169 Trieste, Italy

A metallic system without any further doping was obtained combining, in a bulk film, heterojunctions made by subsequent depositions of C60 and picene layers on Ag(111). This is caused by the formed dipole between the two molecules due to the huge difference in electron affinities and the charge transfer from the substrate. The above situation and the expected molecular geometry have also a role when the heterojunction film is doped with potassium. C60 phases diverse from those observed in bulk C60, especially, a metallic state with continuous alkali doping of the LUMO bands was found. This opens the way towards novel bulk molecular heterojunction structures that may create new electronic phases in strongly correlated molecular materials. The present case appears as the only manner known so far to form a bulk metallic Kx C60 system ($0 < x < 6$) that may evoke the possibility of seeing the awaited dome-shaped region of the doping-temperature phase diagram if the system should show superconductivity.

Many properties of organic superconductors are strongly dependent on the number of charge carriers (doping) put into the lowest unoccupied molecular orbitals (LUMO) bands. The doping is usually chemical and it can be obtained by intercalating alkali metals into the structure of the molecular crystals. Some doped crystals may show a metallic behavior and, sometimes, superconductivity may appear at low temperatures.
The most famous molecular crystal with the highest superconducting critical temperature (Tc) is A3 C60 (A = alkali metal). In these crystals, characterized by three-dimensional arrangements of almost spherical C60 anions, the superconductivity is determined by the competition between localized electronic ground states in fullerenes [1–5]. The absolute Tc observed depends mainly on the electronic structure details related to the molecular orbitals overlap within packing of C60. Tc typically rises with increasing molecular space [1–7] and it is widely accepted that

superconductivity, as observed in high-Tc cuprate superconductors, occurs in connection to the correlation-driven Mott metal-insulator transition over a dome-shaped region of the doping-temperature phase diagram, where the highest Tc is obtained for the so-called “optimum doping” [5].

Differently from the high-Tc superconducting copper oxides families where a continuous doping can be made by cationic substitution, in C60 solid, the electron correlations and the crystal structure permit that only some particular doping phases are possible (phase separation) [8]. Therefore it is hard to follow by doping the dome-shaped region of the doping-temperature phase diagram near the “optimum doping,” which seems to be around 3 electrons/molecule [6].

Here, we demonstrate that growing a heterojunction thin film made by a subsequent depositions of one layer of C60 and one layer of picene, up to a thickness of about 6–7 heterojunction layers on Ag(111), a metallic system is obtained. Moreover, doping the bulk heterojunctions with potassium (K) further metallic states are observed, with density of states (DOS) close to the Fermi level very similar to Kx C60 ($0 < x < 6$) on coinage metals (Au, Ag, and Cu).

Picene and C60 solids doped with potassium are both superconductors with similar Tc (about 18 K) and apparently the same LUMO filling [9]. While for K3 C60, the crystal and electronic structures are well known [2], the situation of superconductivity in K3 picene is quite controversial [9–13].

The two undoped molecular solids show some similarities [1,2,13–15], like comparable correlation energy (Hubbard U ~ 1 eV) and small LUMO band dispersion (0.5 eV). Conversely, they have different work functions (about 5.1 ± 0.1 eV in C60 and 4.6 ± 0.1 eV in picene, see Ref. [16]) and the orbital degeneracy in C60, that causes Jahn-Teller distortion of the molecules in doped compounds [2], is absent in picene. Considering the isolated molecules, they have almost the same ionization potential (I.P.) that is 7.6 eV for C60 [17] and 7.5 eV as we measured for picene (supporting materials), but the electron affinity (E.A.) is quite different, i.e., 2.7 eV for C60 [17] and 0.5 eV for picene [18a,b].

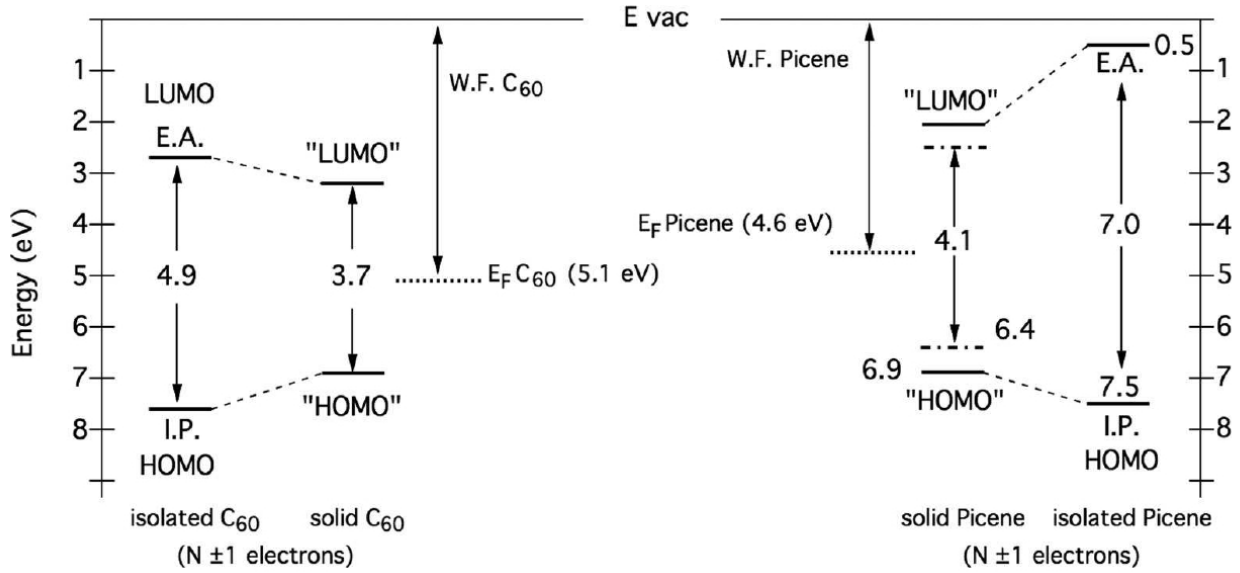

FIG. 1. Energy level diagram for C60 (left) and picene (right). The data for C60 were taken from reference [16], while for picene, we consider the data available in the literature [17] and our measurements. The dashes/dotted line above the “HOMO” for picene is the threshold position for the HOMO band and 4.1 eV is the adiabatic gap as obtained in Ref. [17b,c], see also Ref. [16].

Figure 1 shows an energy level diagram for the isolated C60 and picene molecules and for the respective molecular solids with respect to the vacuum level, according to our measurements and to the data present in the literature. One can expect that the interfacial electronic interactions in heterojunctions aggregates of C60 and picene can induce a ground state distortion of the molecular

charges. The distortion and polarization of the electronic cloud in the picene/C60 heterojunction has the positive pole next to picene and the negative pole next to C60 .

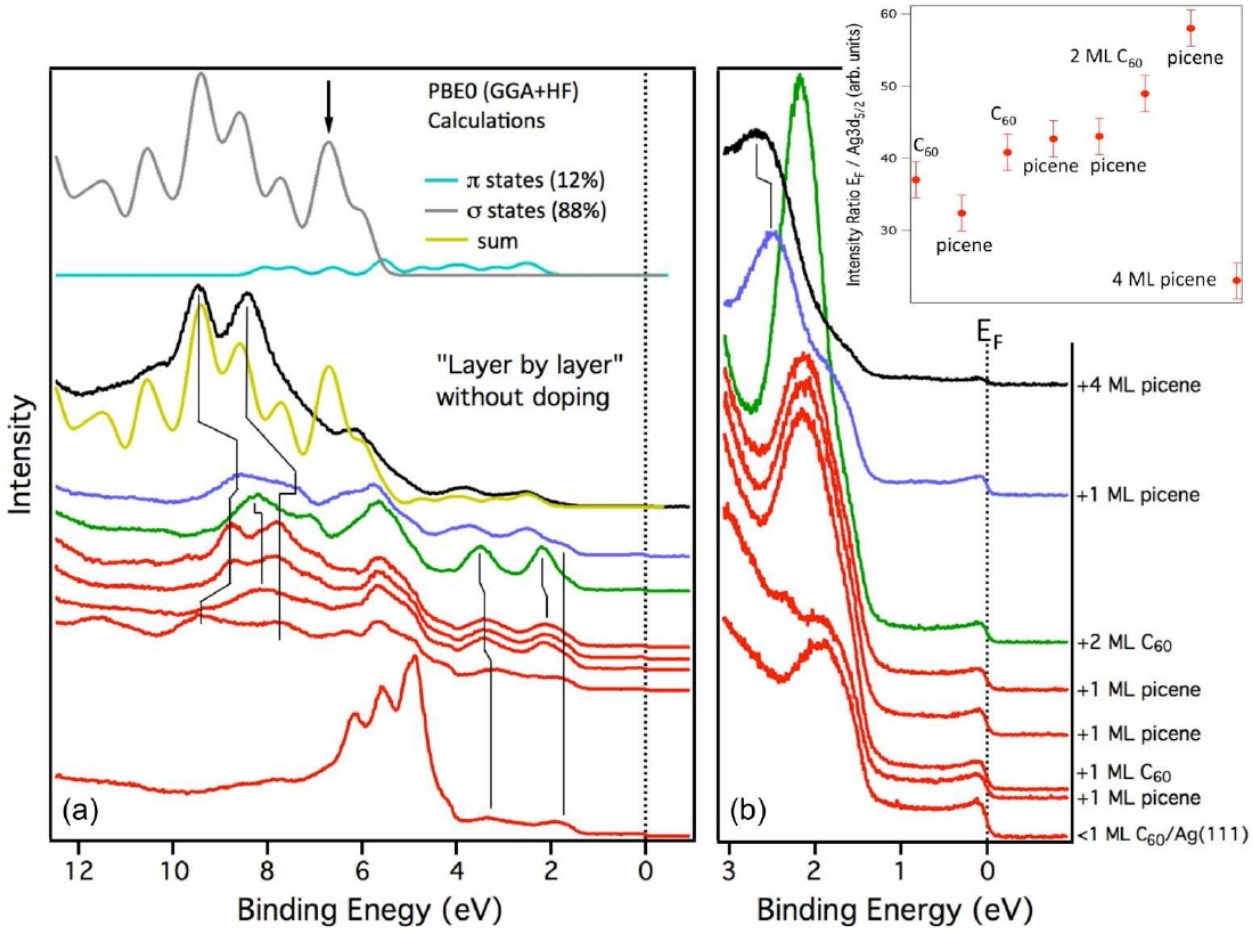

FIG. 2. Valence-band spectra of picene/C60 heterojunctions as a function of the deposition layer of C60 or picene. (a) Extended binding energy region. On top are shown the calculated σ and π DOS of isolated picene molecules with opportune intensity of 88% and 12%, respectively. Their sum is plotted (yellow line) underneath the topmost spectrum (black, 4 ML of picene deposited atop the last heterojunction layer). The small differences in the σ states region (arrow) may be related to symmetry reasons (e.g., the initial state would be odd in our experimental geometry). (b) Binding energy region of the frontier orbitals. Note the presence of the screened HOMO orbital and DOS at EF for each layer of heterojunctions. All the subsequently formed heterojunction layers, starting from the monolayer of C60 /Ag(111), are indicated on the right. (Inset) Intensity ratio EF /Ag 3d5/2, without considering the different escape depths.

Figure 2 shows the valence band photoemission spectra of interfaces formed by depositing alternating layers of C60 and picene molecules, starting from less than a monolayer of C60 on Ag(111) (bottom spectrum, 0.5 ML). This spectrum is characterized mainly by the presence of Ag 4d states with binding energy between 4 and 7 eV, a Fermi edge and the C60 highest occupied molecular orbital (HOMO) and HOMO-1 states on the flat Ag s−p region at 1.8 and 3.3 eV, respectively.

The HOMO and HOMO-1 states appear at lower binding energy with respect to the C60 multilayer due to the metallic screening of the substrate [19]. Some interesting features emerge as the heterojunction system is grown. First, forming the multilayer heterojunctions new molecular-derived states develop and evolve, but the screened HOMO and HOMO-1 states of C60 are always visible at the same binding energy, as it can be seen in particular for the screened HOMO feature after the formation of the last heterojunction, just before covering the surface by 4 ML of picene.

Second, the Fermi level (EF) is always visible, with almost the same intensity, even if the Ag 4d bands are no longer discernible. Eventually, after covering the heterojuctions with 4 ML of picene, the Fermi jump EF is still present although attenuated. Since the intensity at EF remains almost constant when the heterojunctions are formed, the inset of Fig. 2(b) shows that the ratio EF /Ag 3d5/2 (Ref. [16]) increases as the Ag 3d decreases, apart from the last step when the intensity simply attenuates at EF due to the superposition of 4ML of picene. The last spectrum of Fig. 2, apart from the small intensity jump at EF due to the layers underneath, can be considered as the valence band of picene multilayer. Noteworthy, all spectra were collected at normal emission with the light horizontal linear polarization at 40 ° from the surface normal. By looking at the spectral features, we observe that the π peaks are strongly attenuated and the σ part enhanced and well separated in structures. This is a clear indication that the picene multilayer grows with the main molecular axis almost perpendicular to the substrate surface, at variance with the case of picene directly grown on Ag and Au substrates [9,10]. As a confirmation, density functional theory (DFT) simulations of the occupied DOS of isolated picene molecules are shown on top of this spectrum. We weighted π and σ contributions with factors of 0.12 and 0.88, respectively, which correspond to molecules having the main axis at a small angle (~20 °) from the Ag(111) normal. The agreement between the spectrum and the simulation is good, in spite of the fact that the DFT can only approximately describe the true excited spectrum.

Third, as new heterojunction layers are formed starting from the monolayer of C60 /Ag(111), the features appearing in the valence band spectra mainly resemble the typical molecular orbitals of picene or C60 , depending on the termination layer. Some of them shift nonrigidly with respect to the corresponding multilayer spectra (e.g., picene states above 7 eV) caused by both the chemical potential movement and the molecular orbital hybridizations. Other states, like the frontier orbitals HOMO and HOMO-1 near the Fermi level, remain almost fixed.

The presence of a Fermi edge when the heterojunctions are formed, even in multilayer structures, may result from the appearance of an interfacial dipole between picene and C60 , introducing a change in the electronic environment, and is similar to concepts that were put forward for other organic heterojunctions [20–22]. Doped metallic molecular layers, decoupled from the metal surface by one or two sheets of organic molecules, can be assembled without the use of dopants just by forming the proper heterojunctions. Niederhausen et al. [20] investigated C60 (sub)-monolayer films, which are prevented from direct electronic coupling with the Ag(111) substrate by a two-layer thick α-sexithiophene (6T) spacer. The authors unambiguously show that an integer charge transfer from the metal to a fraction of the C60 layer is caused by the interface dipole, while the 6T bilayer remains neutral. Stadtmüller and co-workers [21] showed a gradual filling of the LUMO of 1 ML 3,4,9,10-perylene-tetracarboxylic-dianhydride/Ag(111), which was already partly filled by the Ag substrate, due to a chemisorptive bonding of a further single monolayers of copper(II) phthalocyanine. Finally, a charge transfer from the metal to the hexaaza-triphenylene-hexacarbonitrile layer was observed when it was deposited atop of a monolayer of tris(8-hydroxyquinolinato)aluminum on Ag(111) [22]. Our data indicate a similar trend, but in a multilayer structure of heterojunctions, which offers further flexibility, as also observed for a multilayer of multicomponent N-methyldiazabicyclooctane cation, triptycene, and C60 [23].

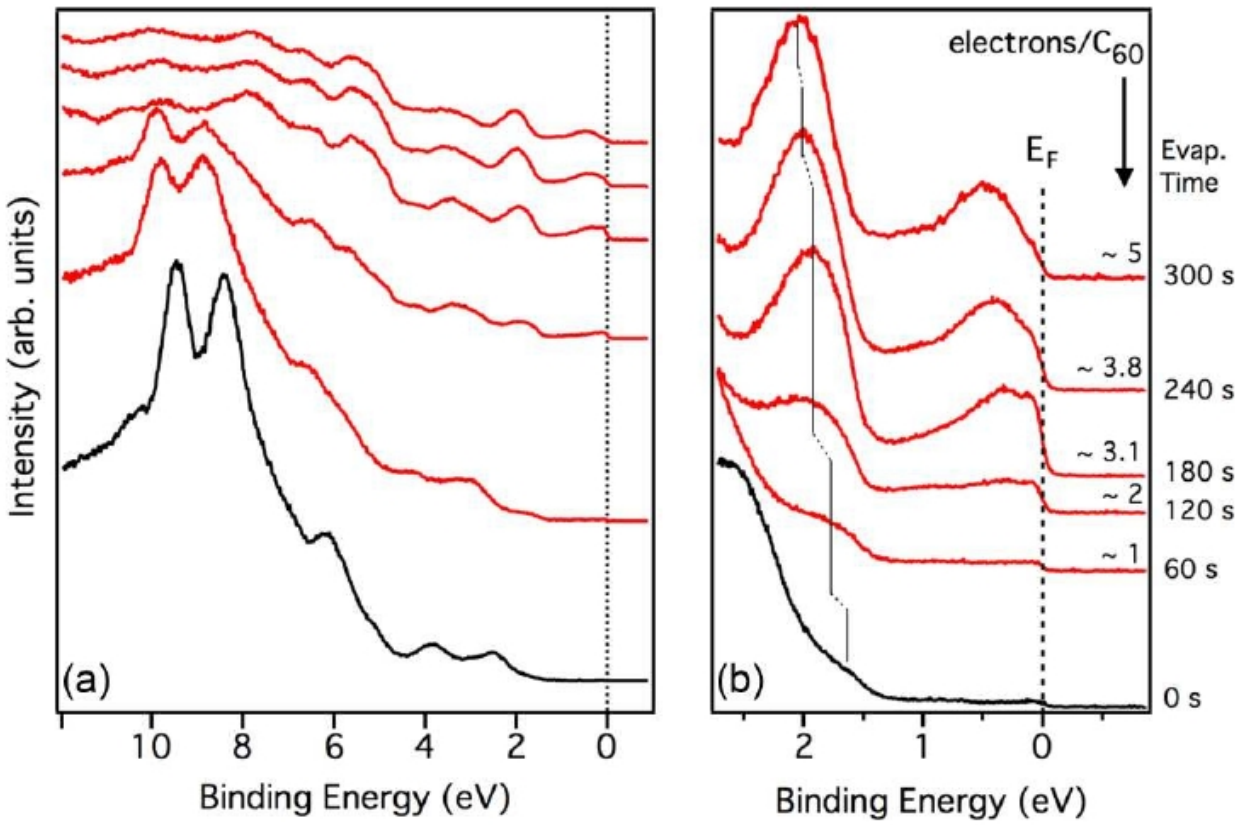

FIG. 3. Valence-band photoemission spectra of the K-doped heterojunctions film starting from the black spectrum where about four monolayer of picene were deposited on top of the seven layers of heterojunction film. (a) Extended binding energy region. (b) Evolution of the frontier orbitals near EF . The expected number of electrons is indicated (see text).

However, to discern whether EF is related to the electronic configuration of this system or to the presence of islands, which leave uncovered areas of Ag, angle-resolved photoemission experiments at different photon energies could be performed in order to observe the presence or not of Ag direct transitions close to the Fermi level. Anyway, the doping of this system with alkali metals seems to be appealing. Due to the high-energy separation between C60 and picene LUMOs, doping the heterojunction with potassium the electrons should fill the C60 LUMO. Near EF , therefore, we should expect to see the same behavior of bulk C60 doped with K. Figure 3 shows the K doping starting from the last spectrum of Fig. 2 (black). Surprisingly, as electrons are donated, the intensity at the EF evolves continuously akin a doped monolayer of C60 on coinage metals [19,24,25]. The number of electrons per C60 molecule, mediated on the few layers investigated with photoemission, can be evaluated from the intensity of the filled LUMO in comparison with the doped monolayer of C60 on Ag(100) [25]. The result, corresponding to a range of about 1 to 5 electrons per C60 molecule, is shown in Fig. 3(b).

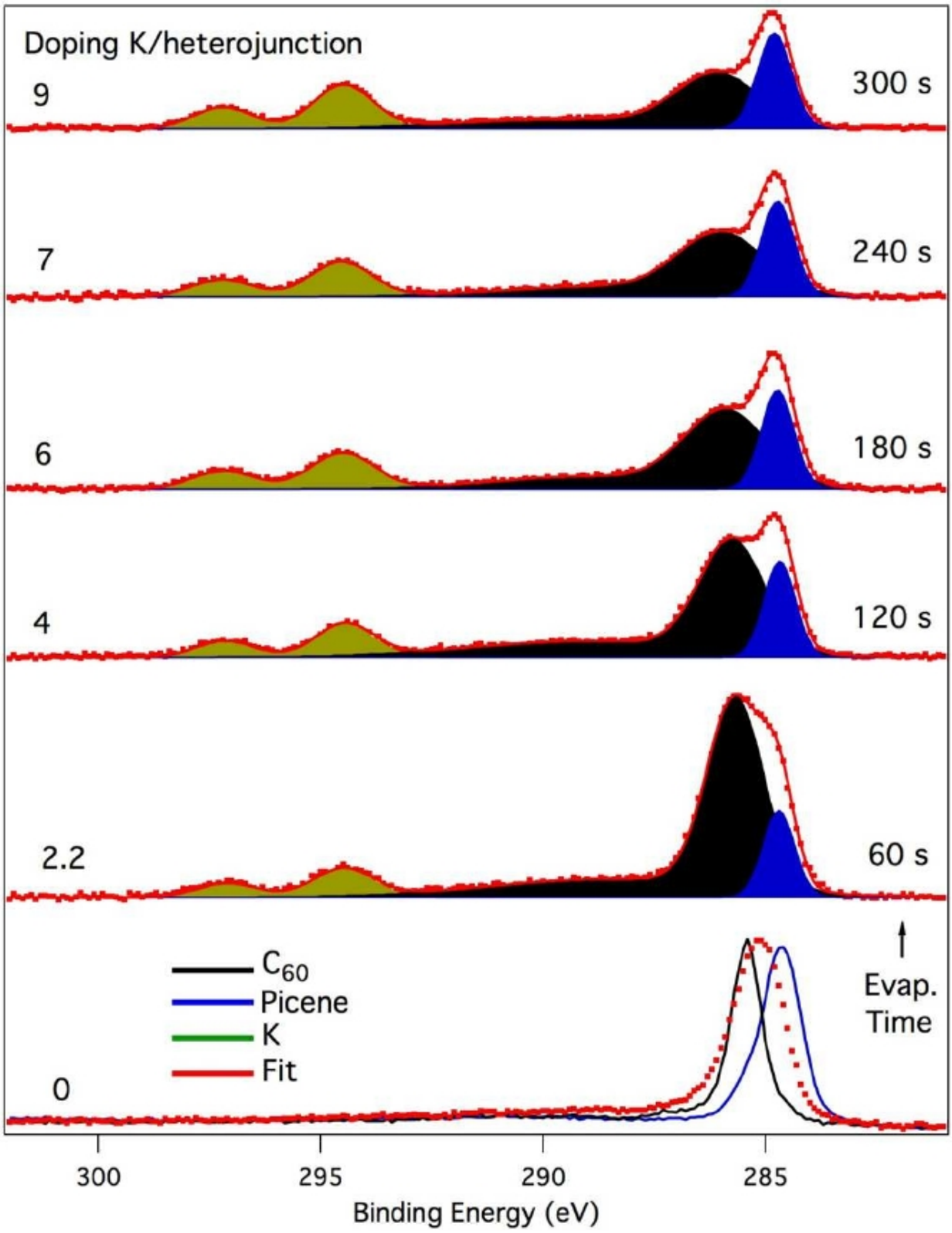

FIG. 4. C1s core level photoemission spectra of undoped thick films (bottom spectra) of C60 (285.5 eV, black line), picene (284.5 eV, blue line), and of picene/C60 heterojunctions (285.0 eV, red points). On top there are the K-doped spectra (red point) with the fit analysis (red line). The green component is the K 2p, the asymmetric black component is the C1s of C60 + loss and the blue component is the C1s of picene. The numbers on the left correspond to the K atoms per heterojuction calculated with the ratio of K 2p and C 1s peak areas. The maximum error in these estimations was ±0.2. The K evaporation time is reported on the right.

That these heterojunctions behave like one monolayer of C60 adsorbed on coinage metals was also confirmed looking at the K2p and C1s core levels plotted in Fig. 4. The spectra of the undoped bulk systems, i.e., C60 multilayer (black line), picene multilayer (blue line) and picene/C60 heterojunctions (red dots), are shown at the bottom of Fig. 4. In particular, the latter is the sum of all the spectra taken while forming several layers of heterojunctions, since these spectra remain in the same position with a similar lineshape (Ref. [16]). This means that EF was pinned during the formation of different heterojunction layers. Moreover, the C1s heterojunction peak is the sum of C60 and picene peaks just shifted in opposite directions by the same amount (0.7 ± 0.1 eV), due to the charge distortion of the formed dipole. On top of these spectra there are the subsequent K doped spectra (red dots) of the multilayer heterojunctions, with the corresponding fits (red line) and the resulting components (potassium K 2p = green, C60 C 1s = black, and picene C 1s = blue). These spectra were plotted as taken. The following features can be highlighted:

(1) The K 2p1/2 and 2p3/2 peaks are always formed by a single component, while on face centered cubic (fcc) bulk C60 compounds, in particular for K3C60 , two components are observed related to octahedral and tetrahedral K atoms [8,26,27]. This immediately tells that the C60 molecules do not form an fcc structure.

(2) Measuring the area of K and C 1s peaks (normalized by their respective photoemission cross sections), the obtained rate of K atoms per heterojunction (C60 + picene) is about two times the electrons per C60 estimated in Fig. 3. Therefore each K atom transfers about 0.5–0.6 electrons to C60 and the remaining electrons on the K atoms form a sort of electrostatic screening continuum around the heterojunctions, which should reduce the intermolecular interactions and, in turn, the magnitude of the interfacial dipole between C60 and picene. The evolution of the C 1s core level seems to confirm this hypothesis, since adding K atoms the two C 1s components start to separate, with the picene always in the same position and the C60 shifting with doping.

To summarize, accurately fabricated picene/C60 hetero-junction films on Ag(111) substrate, may tune the molecular electronic structures in such a way that the electron correlation strength, a key factor in determining the material properties of C60 , can be attenuated. Although here we are not dealing with superconductivity, but only on the electronic structure changes as a function of doping, the superconductivity is a relevant question for this system. Therefore, forming a continuous metallic state in bulk Kx C60 may allow following the possible dome-shaped behavior of Tc as a function of doping. Moreover, it opens the way towards novel molecular heterojunctions that may create new electronic phases in strongly correlated materials [20–23].

Experimental. The experiments were performed at room temperature in ultrahigh vacuum (10−10 mbar) using the experimental chambers of the BaDElPh beamline [28] and of the Micro&Nano-carbon Laboratory (modified VG-Escalab) at the Elettra synchrotron. The clean Ag(111) was prepared by sputtering and annealing cycles until no traces of contaminants were present in the XPS spectra (Mg Kα line) and a clear surface state was visible in the valence-band spectrum. The energy resolution of the XPS measurements was 0.8 eV. C60 and picene molecules were sublimated from degassed Ta crucibles at 300 ℃ and 130 ℃, respectively, and deposited on Ag at room temperature. About 0.5 ML of C60 was obtained by growing a multilayer and then annealing the sample at 270 ℃. The potassium was deposited with the sample at 50 ℃ using a SAES getter evaporator.

The solid valence band photoemission measurements were obtained using a photon energy of 31 eV with the linear horizontal polarization of the light at 40 ° from the sample surface normal. The photoelectrons were collected at normal emission integrating on a ±7° angular window by a SPECS Phoibos 150 mm hemispherical analyzer having a horizontal entrance slit, i.e., in the scattering plane. In these conditions we are collecting spectra in the “even” geometry [29]. The total energy resolution (photons+analyzer) was 30 meV.

For the DFT numerical simulations, we have optimized the geometry with the PBE approximation to the exchange and correlation functional [30] and adopted for a final evaluation of the DOS the hybrid functional PBE0 [31], which was shown to yield a good agreement with many-body calculations and experiments for pentacene and perylene molecules apart from a rigid shift [32]. We used the plane-wave pseudopotential approach [33] with molecules placed in periodically repeated

supercells, with a vacuum separation of 11 Å between adjacent replicas. The DOS shown in Fig. 2 was convoluted with a Gaussian peak having a full with at half maximum of 0.54 eV.

Acknowledgments. This work is partly financed by the Italian MIUR projects FIRB “Supracarbon” RBFR10DAK6 for G.D.S. and FIRB “Nanosolar” RBAP11C58Y for V.A. and A.G. and by the European Community through the ENIAC Joint Undertaking–ERG (Grant Agreement No. 270722-1-ERG) for M.C. C. S. is grateful to the grant of AREA Science Park of Trieste. We thank D. Lonza for technical supports. The critical reading of G. Scoles and E. Tosatti was appreciated.

[1] S. Chakravarty, M.P. Gelfand, and S. Kivelson, Science 254, 970 (1991).
[2] O. Gunnarsson, Alkali-Doped Fullerides: Narrow-Band Solids With Unusual Properties (World Scientific, Singapore, 2004).
[3] Y. Iwasa and T. Takenobu, J. Phys.: Condens. Matter 15, R495 (2003).
[4] P. Durand, G. R. Darling, Y. Dubitsky, A. Zaopo, and M. J. Rosseinsky, Nat. Mater. 2, 605 (2003).
[5] M. Capone, M. Fabrizio, C. Castellani, and E. Tosatti, Phys. Rev. Lett. 93, 047001 (2004); ,Rev. Modern Phys. 81, 943 (2009).
[6] T. Yildirim, L. Barbedette, J. E. Fischer, C. L. Lin, J. Robert, P. Petit, and T. T. M. Palstra, Phys. Rev. Lett. 77, 167 (1996).
[7] A. Y. Ganin, Y. Takabayashi, Y. Z. Khimyak, S. Margadonna, A. Tamai, M. J. Rosseinsky, and K. Prassides, Nat. Mater. 7, 367 (2008).
[8] D.M. Poirier, Appl. Phys. Lett. 64, 1356 (1994).
[9] R. Mitsuhashi, Y. Suzuki, Y. Yamanari, H. Mitamura, T. Kambe, N. Ikeda, H. Okamoto, A. Fujiwara, M. Yamaji, N. Kawasaki, Y. Maniwa, and Y. Kubozono, Nature (London) 464, 76 (2010).
[10] B. Mahns, F. Roth, and M. Knupfer, J. Chem. Phys. 136, 134503 (2012).
[11] M. Caputo, G. Di Santo, P. Parisse, L. Petaccia, L. Floreano, A. Verdini, M. Panighel, C. Struzzi, B. Taleatu, C. Lal, and A. Goldoni, J. Phys. Chem. C 116, 19902 (2012).
[12] P. L. de Andres, A. Guijarro, and J. A. Verges, Phys. Rev. B 83, 245113 (2011).
[13] G. Giovannetti and M. Capone, Phys. Rev. B 83, 134508 (2011).
[14] M. Kim, B. I. Min, G. Lee, H. J. Kwon, Y. M. Rhee, and J. H. Shim, Phys. Rev. B 83, 214510 (2011).
[15] A. Subedi and L. Boeri, Phys. Rev. B 84, 020508(R) (2011).
[16] See Supplemental Material at http://link.aps.org/supplemental/ 10.1103/PhysRevB.90.201401 for the measured work functions of solid C60 and picene, the valence band of picene multilayer and gas phase picene, the C 1s core level photoemission spectra of all the heterojunctions layers formed, the shift in energy of the C 1s of C60 with potassium doping, the growing modes of C60 and picene on Ag(111) and the attenuation of Ag 3d core levels as a function of the heterojunction formation.
[17] D. L. Lichtenberger, K. W Nebesny, C. D. Ray, D. R. Huffman, and L. D. Lamb, Chem. Phys. Lett. 176, 203 (1991); L. S. Wang, J. Conceicao, C. Jin, and R. E. Smalley, ibid. 182, 5 (1991); T. R. Ohno, Y. Chen, S. E. Harvey, G. H. Kroll, J. H. Weaver, R. E. Haufler, and R. E. Smalley, Phys. Rev. B 44, 13747 (1991).
[18] S. Lias, Ionization energy evaluation; J. E. Bartmess, Negative Ion Energetics Data, in NIST Chemistry WebBook, NIST Standard Reference Database No. 69, edited by P. J. Linstrom and W. G. Mallard (National Institute of Standards and Technology, Gaithersburg, MD); N. Sato, K. Seki, and H. Inokuchi, J. Chem. Soc., Faraday Trans. II 77, 1621 (1981); N. Sato, H. Inokuchi, and E. A. Silinsh, Chem. Phys. 115, 269 (1987); F. Roth, M. Gatti, P. Cudazzo, M. Grobosch, B. Mahns, B. Büchner, A. Rubio, and M. Knupfer, New J. Phys. 12, 103036 (2010).
[19] B. W. Hoogenboom, R. Hesper, L. H. Tjeng, and G. A. Sawatzky, Phys. Rev. B 57, 11939 (1998).
[20] J. Niederhausen, P. Amsalem, A. Wilke, R. Schlesinger, S. Winkler, A. Vollmer, J. P. Rabe, and N. Koch, Phys. Rev. B 86, 081411(R) (2012).
[21] B. Stadtmüller, T. Sueyoshi, G. Kichin, I. Kröger, S. Soubatch, R. Temirov, F.S. Tautz, and C. Kumpf, Phys. Rev. Lett. 108, 106103 (2012).

[22] P. Amsalem, J. Niederhausen, J. Frisch, A. Wilke, B. Bröker, A. Vollmer, R. Rieger, K. Müllen, J. P. Rabe, and N. Koch, J. Phys. Chem. C 115, 17503 (2011).
[23] D. V. Konarev, S. S. Khasanov, A. Otsuka, M. Maesato, G. Saito, R. N. Lyubovskaya, Angew. Chem. Int. Ed. 49, 4829 (2010).
[24] P. Rudolf, M. S. Golden, and P. A. Brühwiler, J. Electron Spect. Related Phenom. 100, 409 (1999).
[25] C. Cepek, M. Sancrotti, T. Greber, and J. Osterwalder, Surf. Sci. 454–456, 467 (2000).
[26] D. M. Poirier and J. H. Weaver, Phys. Rev. B 47, 10959 (1993).
[27] A. Goldoni, L. Sangaletti, F. Parmigiani, S. L. Friedmann, Z.-X. Shen, M. Peloi, G. Comelli, and G. Paolucci, Phys. Rev. B 59, 16071 (1999).
[28] L. Petaccia, P. Vilmercati, S. Gorovikov, M. Barnaba, A. Bianco, D. Cocco, C. Masciovecchio, and A. Goldoni, Nucl. Instrum. Methods .Phys. Res., Sec. A 606, 780 (2010).
[29] M. C. Asensio, J. Avila, L. Roca, A. Tejeda, G. D. Gu, M. Lindroos, R. S. Markiewicz, and A. Bansil, Phys. Rev. B 67, 014519 (2003).
[30] J. P. Perdew, K. Burke, and M. Ernzerhof, Phys. Rev. Lett. 77, 3865 (1996).
[31] C. Adamo and V. Barone, J. Chem. Phys. 110, 6158 (1999).
[32] S. Refaely-Abramson, S. Sharifzadeh, N. Govind, J. Autschbach, J. B. Neaton, R. Baer, and L. Kronik, Phys. Rev. Lett. 109, 226405 (2012).
[33] P. Giannozzi et al.., J. Phys.: Condens. Matter 21, 395502 (2009).